ORIENTAL JOURNAL OF CHEMISTRY
An International Open Access, Peer Reviewed Research Journal
www.orientjchem.org
ISSN: 0970-020 X
CODEN: OJCHEG
2025, Vol. 41, No.(6):
Pg. 2158-2165

Physicochemical Optimization of Silver-Doped Amorphous Silica Nanoparticles Toward Efficient Drug Encapsulation and Sustained Release

NUR AIN ATISYA C. M. KHAIRUDDIN[1], NUR ADIBAH ROSLAN[1], ALINA IRWANA MUHAMAD ASRAI[1], MAHANI YUSOFF[2] and MOHD HASMIZAM RAZALI[1,3]*

[1]Faculty of Science and Marine Environment, Universiti Malaysia Terengganu, 21030 Kuala Nerus, Terengganu, Malaysia.
[2]Faculty of Bioengineering and Technology, Universiti Malaysia Kelantan Kampus Jeli, 17600 Jeli,Kelantan, Malaysia.
[3]*Advanced Nanomaterials Research Group, Faculty of Science and Marine Environment, Universiti Malaysia Terengganu, 21030 Kuala Nerus, Terenganu, Malaysia.
*Corresponding author E-mail: mdhasmizam@umt.edu.my

http://dx.doi.org/10.13005/ojc/410628

(Received: October 09, 2025; Accepted: November 27, 2025)

Silica nanoparticles (ASNs) have emerged as promising candidates for drug delivery systems in pharmaceutical applications, owing to their large specific surface area, high biocompatibility, and potential to enhance drug dissolution. Fourier-transform infrared (FTIR) spectroscopy confirmed the presence of characteristic functional groups such as –OH and Si–O–Si, while X-ray diffraction (XRD) analysis verified the amorphous nature of the synthesized silica. Following functionalization with silver (Ag), scanning electron microscopy (SEM) revealed an increase in particle size and a tendency toward agglomeration. This study systematically examined the influence of varying silver concentrations which are 10%, 30%, and 50% on the physicochemical and drug-loading properties of ASNs. The results demonstrated a positive correlation between Ag content and drug loading capacity, with the 50% Ag-doped ASNs exhibiting the highest loading efficiency. The enhancement in drug encapsulation is attributed to the increased density of hydroxyl groups, which facilitate stronger interactions between the drug molecules and the silica matrix. These findings underscore the potential of both ASNs and Ag-doped ASNs as efficient carriers for drug delivery. Moreover, the incorporation of paracetamol, a widely used analgesic and antipyretic agent, demonstrates the system's capability to encapsulate and release small-molecule drugs effectively. Therefore, silver-doped ASNs offer a promising platform for drug delivery applications, including potential use in bone tissue engineering where pain management and inflammation control are critical.

Keywords: Nanocomposites, Biopolymer, Drug delivery, Wound healing.

INTRODUCTION

Amorphous silica nanoparticles (ASNs) have their unique physicochemical characteristics including their huge surface area, variable pore shape, high drug-loading capacity, and exceptional

biocompatibility, have made them a particularly promising material in the field of drug delivery[1]. Their porous structure may hold a wide range of medicinal substances, such as proteins, nucleic acids, and small molecule medicines, and their amorphous nature permits greater flexibility in surface modification[2]. Because of these features, ASNs can be used to achieve prolonged and regulated drug release, improving therapeutic efficacy while lowering the frequency of dosing and decreasing side effects[3]. Biomedical relevance of ASNs is further supported by regulatory bodies' widespread recognition of them as safe (GRAS)[4].

Although a lot of research has concentrated on adding ASNs to composite materials such as hydrogels, scaffolds, and polymeric films in order to increase mechanical strength and replicate biological settings, these materials frequently obscure or change the inherent characteristics of the nanoparticles[5]. The investigation of ASN-specific interactions with pharmacological molecules is complicated by polymer matrices, which might affect drug diffusion behavior, particle dispersion, and degradation rates[6]. It is essential to study ASNs in their pure, powdered form in order to have a more comprehensive and basic understanding of their function as drug delivery carriers. This eliminates the influence of secondary materials and enables researchers to evaluate the direct effects of nanoparticle properties, including surface area, zeta potential, porosity, and surface chemistry, on drug encapsulation and release mechanisms[7].

ASN synthesis in powder form provides a simplified environment for researching the kinetics of drug loading and release. Particle size, shape, and surface functionality can all be affected by synthesis factors like as pH, precursor concentration, reaction duration, and calcination conditions, all of which can be precisely controlled using this method[8]. Researchers can verify the successful synthesis of ASNs and correlate structural features with functional performance using sophisticated characterization techniques like Fourier-transform infrared spectroscopy (FTIR), scanning electron microscopy (SEM), X-ray diffraction (XRD) and thermogravimetric analysis (TGA)[9]. These details are crucial for designing silica-based delivery systems that are optimized for certain medications or target tissues.

Amorphous silica nanoparticles in powder form are synthesized and thoroughly characterized in this work in order to assess their potential as medication carriers for targeted delivery. This work emphasizes the independent role of ASNs in determining drug release behavior by eliminating the production of films or scaffolds. The results of this study offer useful baseline data that can be used in the future for increasingly intricate nanocomposite systems. In the end, the utilization of powder-form ASNs advances our knowledge of drug–nanoparticle interactions and makes it possible to logically develop next-generation delivery systems for biological uses like cancer treatment, bone tissue regeneration, and targeted therapeutic approaches[10].

MATERIALS AND METHODS

Materials

Cetyltrimethylammonium bromide (CTAB), tetraethyl orthosilicate (TEOS), deionized water, distilled water, phosphate-buffered saline (PBS), ethanol (95%), aqueous ammonia (25%), silver nitrate ($AgNO_3$) and paracetamol. Materials were analytical grade and used exactly as it was delivered.

Preparation of ASNs

Sigma-Aldrich, USA, was used as a structure-directing agent. Briefly, water, ethanol, aqueous ammonia (25%), and CTAB in the amounts of 125, 12.5, 9.18, and 2.39 g, respectively, were mixed together in a polypropylene beaker (10 min, 300 rpm, 25°C) until complete CTAB dissolution was achieved. Then, TEOS in the amount of 10.03 g was added and stirred for 2 hours. Subsequently, the mixture was aged at 90°C for 5 days (without stirring). The powder was washed with absolute ethanol, dried at 40°C for 1 h, and calcined at 550°C for 6 h (FCF7SM, Czylok, Poland). The MCM-41 powder was then micronized in a mortar and sieved through sieves to obtain a fraction in the range of 200–500 µm.

Preparation of Ag-ASNs

The amorphous silica type was synthesized using a sol–gel method. Tetraethyl orthosilicate (TEOS, Sigma-Aldrich, USA) was used as a silica source, and cetyltrimethylammonium bromide (CTAB, Sigma-Aldrich, USA) served as a structure-directing agent. Briefly, water, ethanol, aqueous ammonia (25%), and CTAB in the amounts of 125, 12.5, 9.18, and 2.39 g, respectively, were mixed in

a polypropylene beaker (10 min, 300 rpm, 25°C) until complete CTAB dissolution was achieved. Then, TEOS in the amount of 10.03 g and silver nitrate (10%) were added and stirred for 2 hours. Subsequently, the mixture was aged at 90°C for 5 days (without stirring). The powder was washed with absolute ethanol, dried at 40°C for 1 h, and calcined at 550°C for 6 h (FCF7SM, Czylok, Poland). The MCM-41 powder was then micronized in a mortar and sieved through sieves to obtain a fraction in the range of 200–500 µm. This method was repeated with other amounts of silver nitrate (30% and50%).

Sample characterization

The structural, morphological, thermal, and chemical characteristics of the produced amorphous silica nanoparticles (ASNs) and silver-doped versions were verified by the use of many analytical tools. Using a PerkinElmer Spectrum Two spectrometer, Fourier Transform Infrared Spectroscopy (FTIR) was used to establish drug–nanoparticle interactions both before and after paracetamol loading, as well as to identify functional groups including Si–O–Si, Si–OH, and O–H. Using a JEOL JSM-IT100 Scanning Electron Microscope (SEM), surface shape and particle dispersion were examined. A gold coating was added to enhance conductivity. Using a Bruker D8 Advance diffractometer and Cu-Kα radiation, X-ray diffraction (XRD) was used to confirm the amorphous nature of the silica and the existence of silver phases. Thermogravimetric Analysis (TGA) was used to assess thermal behavior and drug content. A PerkinElmer TGA 4000 was used to quantify weight changes under nitrogen from 30°C to 800°C. Finally, a Shimadzu UV-1800 spectrophotometer was used for UV-Visible Spectrophotometry in order to monitor the drug release profile at 243 nm using a standard calibration curve and assess the drug loading efficiency. Every characterization method confirmed the nanoparticles' promise as powdered drug delivery systems by offering important new information about their structure–function relationship.

Drug loading into nanoparticles

A mixture consisting of 0.5 mL of phosphate-buffered saline (PBS), 2.5 mL of 10 ppm paracetamol solution, and 5 mg of amorphous silica nanoparticles (ASNs) was prepared and stirred continuously for 24 h at room temperature to ensure optimal interaction between the drug molecules and the nanoparticle surfaces. After the incubation period, the sample was centrifuged at 12,000 rpm for approximately 6 min to separate the nanoparticles from the residual free (unloaded) paracetamol present in the supernatant. The recovered nanoparticle pellet was gently rinsed with distilled water to eliminate any leftover unbound drugs. Following the procedure modified by SaharPorrang (2021), the concentration of the unloaded paracetamol in the supernatant was then measured using a UV-Visible spectrophotometer set to a detection wavelength of 243 nm[11]. The following formula was used to determine the drug loading efficiency (DLE):

$$\text{Drug loading efficiency (\%)} = \frac{C_1 - C_f}{C_i} \times 100\% \quad (1)$$

Where C_i is the initial concentration of paracetamol (10 ppm) and C_f is the final concentration of the drug remaining in the supernatant after 24 hours.

***In vitro* drug release**

Amorphous silica nanoparticles containing paracetamol were reconstituted in four mL of phosphate-buffered saline (PBS) and tested for drug release in vitro under two distinct pH settings: 5.4 and 7.4, which correspond to acidic and physiological environments, respectively. To replicate physiological temperature, the dispersions were kept in a shaker incubator set at 37°C. To maintain sink conditions, an equivalent volume of fresh PBS was supplied after the samples were centrifuged at certain times to separate the supernatant containing the released paracetamol. Using a UV-Visible spectrophotometer set to a detection wavelength of 243 nm, the concentration of paracetamol released into the supernatant was determined using a technique modified by SaharPorrang (2021)[11]. The following formula was used to determine the percentage of medication released at each time point:

$$\text{Drug release (\%)} = \frac{\text{Amount of drug released at time} \times 100}{\text{Initial amount of drug encapsulated in the sample}} \quad (2)$$

RESULT AND DISCUSSION

The FTIR spectra of the powder samples as shown in Fig. 1, comprising amorphous silica and silver-doped amorphous silica nanoparticles, displays characteristic absorption bands typical of silica-based materials. A broad band around 3400 cm^{-1} corresponds to O–H stretching vibrations from surface hydroxyl groups and adsorbed water,

indicating strong hydrogen bonding interactions[12], while a peak near 1630 cm^{-1} is attributed to H–O–H bending vibrations of molecular water[13]. A prominent absorption band observed at approximately 1100 cm^{-1} represents the asymmetric stretching of Si–O–Si bonds, confirming the formation of a siloxane network[14]. Additional peaks near 800 cm^{-1} and 460 cm^{-1} correspond to symmetric Si–O–Si stretching and Si–O bending vibrations, respectively, supporting the presence of an amorphous tetrahedral silica structure[15]. In the silver-doped samples, slight shifts and changes in intensity of the Si–O–Si bands were observed, which suggest partial substitution or structural influence of silver ions on the silica framework[16]. Moreover, the appearance of weak bands between 500–600 cm^{-1} may be attributed to Ag–O bond formation, indicating successful incorporation of silver into the silica matrix[17]. These spectral modifications collectively confirm the effective doping of silver and structural alteration of the base silica network.

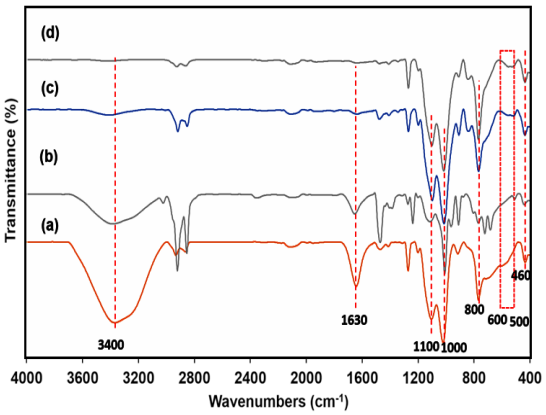

Fig. 1. FTIR spectra of (a) ASNs Powder (b) Ag-ASNs 10% Powder (c) Ag-ASNs 30% Powder (d) Ag-ASNs 50% Powder

Figure 2 shows the XRD patterns for four powder samples which were ASNs, 10% Ag-ASNs, 30% Ag-ASNs, and 50% Ag-ASNs. Since sol-gel generated silica typically lacks long-range atomic order, all samples exhibit a broad peak centeredaround 2θ = 21.92°, demonstrating the amorphous nature of silica[14]. Additional peaks in the silver-doped samples are seen at 2θ values of roughly 38.12°, 44.28°, 64.44°, and 77.40°. These values correspond to the (111), (200), (220), and (311) planes of the metallic silver face-centered cubic (FCC) structure, as listed in JCPDS No. 04-0783[18]. Increased crystallinity and effective silver nanoparticle incorporation into the silica matrix are suggested by the sharpening and intensifying of these silver peaks, especially in the 50% Ag-ASNs sample[17]. A dual-phase structure where silica acts as the host matrix and silver develops embedded crystalline domains is shown by the presence of a broad amorphous silica peak and clear crystalline silver reflections. This structural combination is beneficial for drug delivery applications because silver's bioactive and antibacterial qualities improve therapeutic functionality, while amorphous silica's large surface area facilitates drug loading[17].

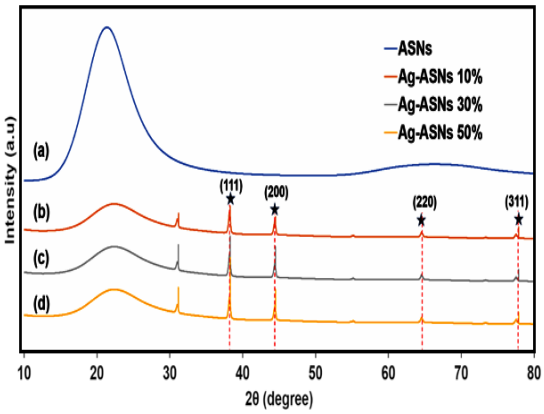

Fig. 2. XRD patterns of (a) ASNs Powder (b) Ag-ASNs 10% Powder (c) Ag-ASNs 30% Powder (d) Ag-ASNs 50% Powder

Figure 3 presents the SEM micrographs of pure and silver-doped amorphous silica nanoparticles (ASNs). The pure ASNs in Fig. 3(a) exhibit smooth, mostly spherical particles with minimal aggregation, consistent with sol-gel-synthesized silica as reported by Ramesh *et al.,* (2016)[19]. In Fig. 3(b), the 10% Ag-ASNs sample retains its spherical shape but shows a rougher surface and the appearance of bright spots, indicating successful silver incorporation. Mild agglomeration is also observed. As silver content increases to 30%, the SEM micrograph reveals more pronounced surface roughness, irregular shapes, and intensified particle aggregation, with brighter regions suggesting a more widespread silver distribution (Fig. 3(c). For the 50% Ag-ASNs sample (Fig. 3(d), particles appear highly rough, irregular, and heavily agglomerated, with strong clustering effects due to the high silver concentration. These observations suggest that increasing silver doping alters the surface morphology of ASNs, leading to greater structural distortion and aggregation, as supported by Xiao *et al.,*(2019)[20].

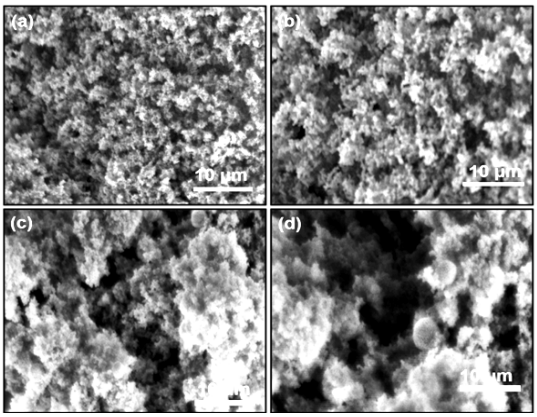

Fig. 3. SEM micrographs of (a) ASNs powder (b) Ag-ASNs 10% powder (c) Ag-ASNs 30% powder (d) Ag-ASNs 50% powder

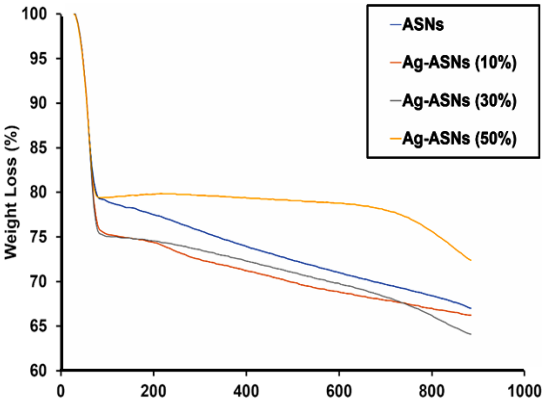

Fig. 4. TGA analysis of (a) ASNs Powder (b) Ag-ASNs 10% Powder (c) Ag-ASNs 30% Powder (d) Ag-ASNs 50% Powder

Figure 4 displays the TGA curves of pure amorphous silica nanoparticles (ASNs) and silver-doped variations (Ag-ASNs) with 10%, 30%, and 50% silver content. The measurements were made between room temperature and 900°C. There are two main stages of weight reduction in every sample. The elimination of physically adsorbed water causes an initial weight loss of about 4.5% for pure ASNs below 100°C[14]. The breakdown of remaining organic precursors such CTAB, TEOS, and APTES causes a weight loss of 10.2% between 200°C and 550°C[21]. The silica matrix's thermal adaptability is seen by the curve stabilizing at about 600°C[15]. The profile of the 10% Ag-ASNs sample is similar, with approximately 5.1% weight loss below 90°C as a result of moisture and 9.5% organic breakdown between 220°C and 500°C, followed by stabilization above 600°C. Improved resistance at intermediate silver content is suggested by the 30% Ag-ASNs sample, which exhibits a somewhat lower moisture loss (4.3%) but a more noticeable 11.6% weight loss from 210°C to 530°C, reaching thermal stability around 640°C[17]. The 50% Ag-ASNs sample, on the other hand, shows a total weight loss of 14.7% between 200°C and 750°C, with a higher initial weight loss (6.2%) below 100°C, perhaps as a result of increased surface moisture, and a broader, slower degradation phase. The fact that stability is only attained until 700°C suggests that increased silver loading causes more complicated breakdown behavior and delays stabilization[16]. Overall, all samples show thermal stability over 600°C, and the stability range and decomposition pattern are influenced by silver doping.

Paracetamol, a widely used analgesic and antipyretic drug with pH-dependent solubility[11]. It was loaded into the nanoparticles via a simple mixing method at room temperature. The unloaded paracetamol was removed by centrifugation, and the loading efficiency was calculated by measuring the concentration of the remaining free drug using UV–Vis spectrophotometry. The percentage of paracetamol loading and encapsulation efficiency was summarized and presented in Table 1.

At pH 7.4 and 5.4, which mimic normal physiological and slightly acidic pathological conditions, respectively, the *in vitro* drug release behavior of amorphous silica nanoparticles (ASNs) loaded with paracetamol and silver-doped ASNs (Ag-ASNs 10%) was examined. Both samples displayed an alternating release profile, as seen in Figure X, with a slower sustained release phase over the course of 24 h after an initial burst. The pH-sensitive character of the nanoparticle system was demonstrated at all time intervals by the fact that drug release was greater in acidic circumstances (pH 5.4) than in neutral pH (7.4). The increased solubility and hydrophilicity of paracetamol, which results from the protonation of its functional groups at low pH and accelerates diffusion out of the nanoparticle matrix, are responsible for this greater release in acidic media[22].

Ag-ASNs 10% showed more cumulative drug release than pure ASNs in both formulations at both pH values, however the difference became more noticeable over time at pH 5.4. This could be because the addition of silver improved drug loading and promoted more diffusion by creating a

rougher surface morphology and more porosity[16]. Additionally, silver may cause a minor disruption in the silica network, which would impair drug-matrix interactions and speed up release[1]. These findings imply that 10% silver doping maintains the structural integrity of ASNs while also enhancing their ability to transport drugs in acidic environments. The promise of Ag-ASNs as an efficient nanocarrier device for site-specific paracetamol administration is highlighted by the combination of pH sensitivity and controlled release[12].

Table 1: Silica nanoparticles drug loading and encapsulation efficiency

Types of Nanoparticles	Drug Loading %	Encapsulation %
ASNs	0.49	97.74
Ag-ASNs 10%	0.49	97.02

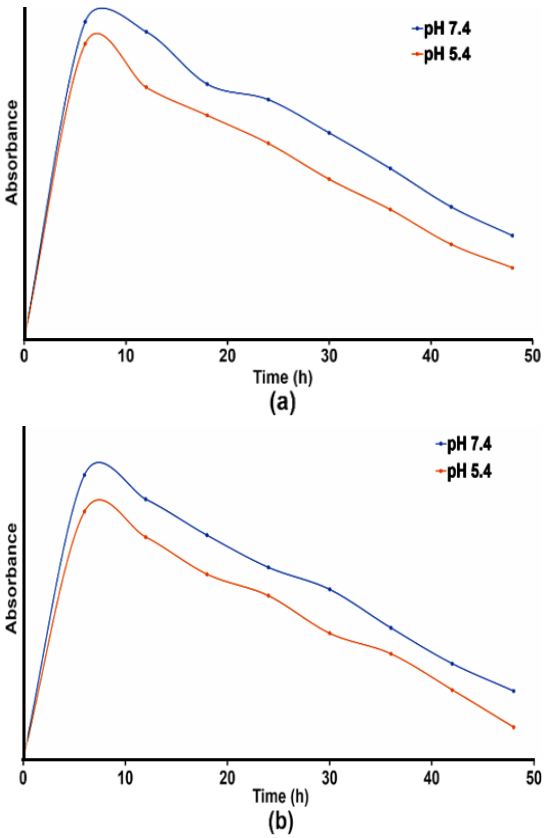

Fig. 5. Drug release profile of (a) amorphous silica nanoparticles (ASNs) and (b) silver doped amorphous silica nanoparticles (Ag-ASNs 10%)

The efficiency of the nanocarriers in encapsulating the drug was assessed by measuring the drug loading (DL%) and encapsulation efficiency (EE%) of paracetamol into amorphous silica nanoparticles (ASNs) and 10% silver-doped ASNs (Ag-ASNs). Despite the little variation in the amount of drug retained, both ASNs and 10% Ag-ASNs showed similar drug loading capabilities of roughly 0.49%, as indicated in Table X. This is to be expected since the drug-to-carrier ratios were almost the same in both systems due to the use of the same initial drug concentration (0.025 mg of paracetamol) and nanoparticle mass (5 mg). The comparable loading percentages imply that the total amount of drug physically retained inside the nanoparticle matrix is not much changed by 10% silver doping[1]. However, there was a slight but noticeable variation in the encapsulation efficiency (EE%). 10% Ag-ASNs had an EE% of 97.02%, while ASNs had an EE% of 97.74%. The addition of silver ions may have altered the system's surface or structure, which would explain the small drop in EE% for the silver-doped system. The interaction between paracetamol molecules and the internal silica surface during loading may be reduced by silver doping, which can alter pore connectivity and enhance surface roughness[19]. Silver may also change the nanoparticles' hydrophilicity or surface charge, which could have an impact on drug-nanocarrier interactions[23]. These results are consistent with earlier research showing that, even in cases where the general structure stays the same, doping materials such as silver can affect drug encapsulation by altering surface chemistry[12].

CONCLUSION

In this study, the sol-gel method was effectively used to produce and completely characterize powdered amorphous silica nanoparticles (ASNs) and silver-doped ASNs (Ag-ASNs). Excellent drug encapsulation efficiency and pH-responsive drug release behavior were displayed by both nanomaterials; 10% Ag-ASNs showed somewhat improved release performance in acidic environments. The amorphous silica framework was preserved although significant morphological and chemical changes were brought about by the integration of silver, according to structural and surface investigations. The silver-doped system's large surface area, adjustable porosity, and bioactive potential demonstrate its suitability for intelligent drug administration. According to these results, ASNs and Ag-ASNs may be useful carriers for the targeted and regulated administration of medicinal substances, with possible uses in bone tissue regeneration and

localized therapy. While this study demonstrates the successful physicochemical optimization of silver-doped amorphous silica nanoparticles for improved drug encapsulation and sustained release, comprehensive biological evaluations remain necessary. Future work should include systematic cytotoxicity assays, hemocompatibility tests, and long-term biomedical safety assessments to further validate the suitability of these nanoparticles for therapeutic applications. Such studies will be essential to bridge the gap between laboratory-scale optimization and potential clinical translation.

ACKNOWLEDGEMENT

We thank Universiti Malaysia Terengganu for providing funding support for this project (UMT/PPP/IPRG/2022/55333).

Conflict of interest

The author declare that we have no conflict of interest.

REFERENCES

1. Slowing, I. I.; Vivero-Escoto, J. L.; Wu, C.-W., & Lin, V. S.-Y., Mesoporous silica nanoparticles as controlled release drug delivery and gene transfection carriers., *Adv. Drug Deliv. Rev.*, **2008**, *60*(11), 1278–1288.
2. Tang, F.; Li, L., & Chen, D., Mesoporous silica nanoparticles: synthesis, biocompatibility and drug delivery., *Adv. Mater.*, **2012**, *24*(12), 1504–1534.
3. Vallet-Regí, M.; Balas, F., & Arcos, D., Mesoporous materials for drug delivery., *Angew. Chem. Int. Ed.*, **2007**, *46*(40), 7548–7558.
4. Baeza, A., Mesoporous silica nanoparticles in drug delivery and biomedical applications., *Microporous Mesoporous Mater.*, **2015**, *200*, 1–10.
5. Bharti, C., Polymeric films as a promising carrier for bioactive drugs., *Asian J. Pharm. Sci.*, **2015**, *10*(4), 276–290.
6. He, Q.; Zhang, Z.; Gao, F.; Li, Y., & Shi, J. *In vivo* biodistribution and urinary excretion of mesoporous silica nanoparticles: effects of particle size and PEGylation., *Small.*, **2011**, *7*(2), 271–280.
7. Rosenholm, J. M.; Sahlgren, C., & Lindén, M. Towards multifunctional, targeted drug delivery systems using mesoporous silica nanoparticles., *Nanoscale.*, **2010**, *2*(10), 1870–1883.
8. Mamaeva, V., Mesoporous silica nanoparticles as drug delivery systems for targeted cancer therapy: recent trends and challenges., *Nanoscale.*, **2013**, *5*(7), 2353–2364.
9. Wu, S. H.; Hung, Y., & Mou, C. Y., Mesoporous silica nanoparticles as nanocarriers., *Chem. Commun.*, **2011**, *47*(36), 9972–9985.
10. Izquierdo-Barba, I., Nanostructured hybrid materials for bone regeneration., *Adv. Healthcare Mater.*, **2011**, *4*(5), 748–764.
11. Porrang, S.; Rahemi, N.; Davaran, S.; Mahdavi, M., & Hassanzadeh, B., Preparation and in-vitro evaluation of mesoporous biogenic silica nanoparticles obtained from rice and wheat husk as a biocompatible carrier for anti-cancer drug delivery., *European Journal of Pharmaceutical Sciences.*, **2021**, *163*, 105866.
12. Tang, F.; Li, L., & Chen, D., Mesoporous silica nanoparticles: synthesis, biocompatibility and drug delivery., *Advanced Materials.*, **2012**, *24*(12), 1504–1534.
13. Wu, S. H.; Hung, Y., & Mou, C. Y., Mesoporous silica nanoparticles as nanocarriers., *Chemical Communications.*, **2011**, *47*(36), 9972–9985.
14. Rahman, I. A & Padavettan, V., Synthesis of silica nanoparticles by sol-gel: size-dependent properties, surface modification, and applications in silica–polymer nanocomposites., *Journal of Nanomaterials.*, **2012**, Article ID 132424.
15. Iler, R. K., The chemistry of silica, A Wiley-Interscience publication. Willey and Sons, New York., **1979**, 665-676.
16. Wang, Y.; Zhao, Q.; Han, N.; Bai, L.; Li, J.; Liu, J., & Wang, S., Mesoporous silica nanoparticles in drug delivery and biomedical applications., *Microporous and Mesoporous Materials.*, **2015**, *200*, 1–10.
17. Chen, G. S.; Chen, C. N.; Tseng, T. T.; Wei, M. H.; Hsieh, J. H., & Tseng, W. J., Synthesis, characterization, and antibacterial activity of silver-doped silica nanocomposite particles., *Journal of Nanoscience and Nanotechnology.*, **2011**, *11*(1), 90-97.
18. JCPDS File No. 04-0783. Joint Committee on Powder Diffraction Standards, International Centre for Diffraction Data.

19. Dubey, R. S.; Rajesh, Y. B. R. D., & More, M. A., Synthesis and characterization of SiO2 nanoparticles via sol-gel method for industrial applications., *Materials Today: Proceedings*., **2015**, *2*(4-5), 3575-3579.
20. Munir, T.; Mahmood, A.; Peter, N.; Rafaqat, N.; Imran, M., & Ali, H. E., Structural, morphological and optical properties at various concentration of Ag doped SiO_2-NPs via sol gel method for antibacterial and anticancer activities., *Surfaces and Interfaces*., **2023**, *38*, 102759.
21. Vazquez, N. I.; Gonzalez, Z.; Ferrari, B., & Castro, Y., Synthesis of mesoporous silica nanoparticles by sol–gel as nanocontainer for future drug delivery applications., *Boletín de la Sociedad Española de Cerámica y Vidrio*., **2017**, *56*(3), 139-145.
22. Kanniyappan, H.; Jose, J.; Chakraborty, S.; Ramasamy, M.; &Muthuvijayan, V., pH-responsive drug release from positively charged mesoporous silica nanoparticles and their potential for anticancer drug delivery., *Journal of the Australian Ceramic Society*., . **2023**, *59*(1), 207-220.
23. Trewyn, B. G.; Slowing, I. I.; Giri, S.; Chen, H. T., & Lin, V. S. Y., Synthesis and functionalization of a mesoporous silica nanoparticle-based delivery system for carrying Doxorubicin., *Small*., **2007**, *3*(5), 936–943.